# $K_2AuPS_4$, $Tl_2AuPS_4$, $K_2AuAsS_4$, and $KAu_5P_2S_8$: Syntheses, Structures, and Properties of Quaternary Gold Thiophosphate and Thioarsenate Compounds

**Sandra Löken and Wolfgang Tremel***

Institut für Anorganische Chemie und Analytische Chemie der Johannes-Gutenberg-Universität, Becherweg 24, D-55099 Mainz, Germany

Received July 16, 1997

**Keywords:** Gold / Chalcogenide / Flux reaction / Structure determination / Metal-metal bonding

The novel compounds $K_2AuPS_4$ (**1**), $Tl_2AuPS_4$ (**2**), $K_2AuAsS_4$ (**3**), and $KAu_5P_2S_8$ (**4**) have been synthesized by direct reaction of the elements with a molten alkaline polythiophosphate(arsenate) flux at 550°C. The crystal structures of these compounds have been determined by single-crystal X-ray diffraction techniques. **1**, **2**, and **3** crystallize in the monoclinic space group $P2_1/m$. The structures of **1**, **2**, and **3** consist of infinite, one-dimensional anionic chains running along the crystallographic *b* axis. The chains are separated by potassium or thallium ions. Neighbouring Au atoms are bridged by $MS_4^{3-}$ tetrahedra (M = P, As) in a *trans* orientation. Compound **4** crystallizes in the space group $P2_1/c$. The anionic chains of **4** are built up from linear $AuS_2$ dumbbell units and $PS_4^{3-}$ tetrahedra. The chains extend along the $[1\bar{1}0]$ and $[1\bar{1}0]$ direction and are separated by charge balancing $K^+$ cations. Each of the compounds was investigated by differential thermal analysis, FT-IR, and solid-state UV/Vis diffuse reflectance spectroscopy.

## Introduction

Most transition metals react with chalcogen or chalcogen-containing compounds to give transition-metal chalcogenides. These compounds have been the subject of numerous studies during the past decades because of their intriguing electronic and chemical properties such as superconductivity[1], charge-density wave behavior[2] and intercalation chemistry[3], which are imparted by the low-dimensional character of the early transition-metal compounds. On the right-hand side of the Periodic Table, transition-metal chalcogenides prefer three-dimensional structures akin to those of pyrites or marcasite. Several papers on this matter have recently been published[4], while a general explanation for these observations was advanced long ago by Hoffmann and Zheng[5]. When we move across the transition series, the d bands decrease in energy and become narrower. At the same time, the band filling increases. These two competing factors determine the trend in the Fermi level: It falls as one moves to electron-rich transition metals. If bands of Q−Q (Q = chalcogen) σ and σ* character are superimposed on these transition-metal d bands, the Fermi level will be above the bands with Te−Te σ* character for the early transition metals, i.e. on the left-hand side of the Periodic Table, but below for the late transition metals, i.e. on the right-hand side. The result is a gradual increase of Q−Q bonding in metal chalcogenides as we move across the transition-metal series from left to right. Compounds at the crossover point are most interesting from a theoretical point of view, because in these cases a straightforward prediction of their electronic properties by a formal assignment of oxidation states becomes impossible. In the simple binary compounds, one can reach the crossover point by varying the metal or the chalcogen components. As far as the metals are concerned, chalcogenides of the coinage metals are definitely such borderline cases. For gold tellurides such as $AuTe_2$, a compound with a very distorted $CdI_2$ structure, even more ambiguities arise, as now the metal (Pauling elec-

Figure 1. Unit cell view down the a) [010] axis, b) [100] axis for $K_2AuAsS_4$ (**2**) (medium grey spheres: As, black spheres: Au, open spheres: S, large grey spheres: K)

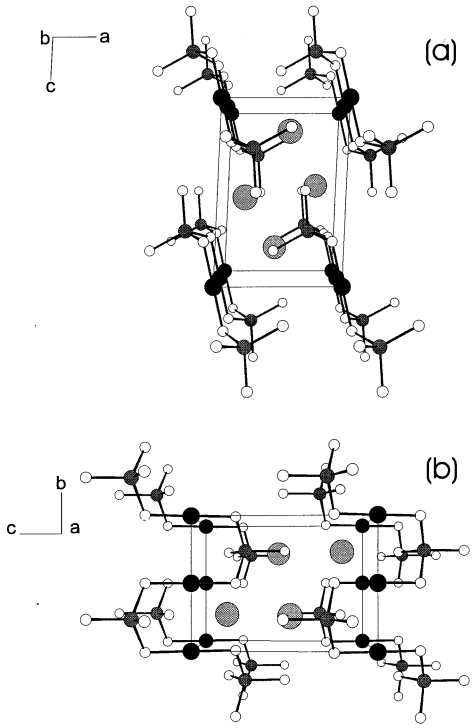


  1434−1948/98/0202−0283 $ 17.50+.50/0 

Table 1. Selected bond lengths [Å] and angles [°] for $K_2AuPS_4$ (**1**), $Tl_2AuPS_4$ (**2**), and $K_2AuAsS_4$ (**3**) (with standard deviations in parentheses)

| Atoms | $K_2AuPS_4$ | $Tl_2AuPS_4$ | $K_2AuAsS_4$ |
|---|---|---|---|
| | Distances | | |
| Au−Au | 3.364(0) × 2 | 3.335(0) × 2 | 3.430(0) × 2 |
| Au−S1 | 2.298(2) × 2 | 2.300(3) × 2 | 2.292(4) × 2 |
| Au−A2 | 3.810(4) × 2 | 3.430(1) × 2 | 3.823(6) × 2 |
| P−S1 | 2.082(4) × 2 | 2.079(5) × 2 | 2.185(5) × 2 |
| P−S2 | 2.013(5) | 2.026(7) | 2.139(7) |
| P−S3 | 2.018(5) | 2.020(7) | 2.142(7) |
| mean P(As)−S | 2.049 | 2.051 | 2.163 |
| A1−S1 | 3.413(4) × 2 | 3.368(3) × 2 | 3.497(7) × 2 |
| A1−S1 | 3.307(4) × 2 | 3.356(4) × 2 | 3.334(7) × 2 |
| A1−S2 | 3.176(5) | 3.244(5) | 3.178(9) |
| A1−S3 | 3.456(1) × 2 | 3.415(1) × 2 | 3.511(2) × 2 |
| A1−S3 | 3.319(5) | 3.340(5) | 3.342(8) |
| A1−S3 | 3.202(5) | 3.143(5) | 3.254(8) |
| A2−S1 | 3.446(4) × 2 | 3.401(4) × 2 | 3.489(7) × 2 |
| A2−S2 | 3.366(0) × 2 | 3.336(0) × 2 | 3.431(0) × 2 |
| A2−S2 | 3.212(6) | 3.027(5) | 3.22(1) |
| A2−S3 | 3.314(5) | 3.429(5) | 3.270(9) |
| mean A−S | 3.347 | 3.329 | 3.386 |
| | Angles | | |
| S1−Au−S1 | 180.00(7) | 180.0(1) | 180.0(1) |
| P(As)−S1−Au | 107.0(1) | 110.4(2) | 106.2(2) |
| S1−P(As)−S1 | 111.2(2) | 112.1(2) | 111.0(2) |
| S2−P(As)−S1 | 111.3(1) × 2 | 111.0(2) × 2 | 111.6(2) × 2 |
| S3−P(As)−S1 | 103.6(1) × 2 | 103.9(2) × 2 | 103.3(2) × 2 |
| S3−P(As)−S2 | 115.2(2) | 114.6(3) | 115.4(3) × 2 |

Figure 2. $KAu_5P_2S_8$ (**4**) viewed down the [110] axis (medium grey spheres: K, open spheres: Au, $PS_4$ tetrahedra), Au−Au short contacts are shown by dashed lines

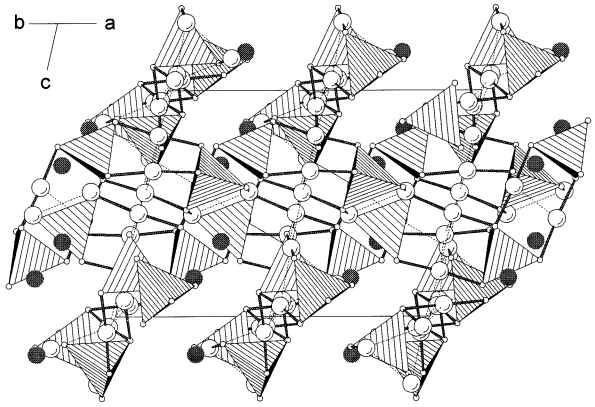


Figure 3. Anionic structure of $KAu_5P_2S_8$ (**4**, open spheres: Au, $PS_4$ tetrahedra)

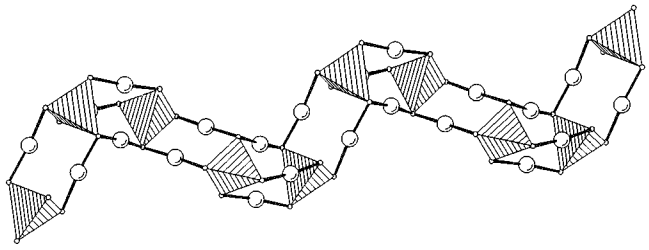

Table 2. Selected bond lengths [Å] and angles [°] for $KAu_5P_2S_8$ (**4**) (with standard deviations in parentheses)

| Atoms | Distance | Atoms | Distance |
|---|---|---|---|
| Au1−Au2 | 3.393(3) | Au5−S7 | 2.31(1) |
| Au1−Au3 | 2.962(3) | mean Au−S | 2.31 |
| Au1−Au3 | 3.033(3) | K1−S1 | 3.43(2) |
| Au1−Au4 | 3.138(3) | K1−S2 | 3.21(2) |
| Au1−Au5 | 3.204(3) | K1−S4 | 3.24(2) |
| Au2−Au2 | 3.148(3) | K1−S6 | 3.47(2) |
| Au2−Au3 | 3.043(3) | K1−S7 | 3.29(2) |
| Au3−Au4 | 3.121(3) | K1−S8 | 3.71(2) |
| Au5−Au5 | 3.193(3) | K1−S8 | 3.42(2) |
| mean Au−Au | 3.137 | mean K−S | 3.40 |
| Au2−K1 | 3.71(1) | S1−P1 | 1.98(2) |
| Au1−S4 | 2.31(1) | S2−P1 | 2.03(2) |
| Au1−S7 | 2.31(2) | S4−P1 | 2.16(2) |
| Au2−S4 | 2.32(1) | S5−P1 | 2.06(2) |
| Au2−S5 | 2.30(1) | S3−P2 | 1.99(2) |
| Au3−S1 | 2.34(1) | S6−P2 | 2.06(2) |
| Au3−S3 | 2.30(1) | S7−P2 | 2.12(2) |
| Au4−S2 | 2.30(1) | S8−P2 | 2.07(2) |
| Au4−S8 | 2.32(1) | mean S−P | 2.06 |
| Au5−S6 | 2.30(2) | | |
| **Atoms** | **Angle** | **Atoms** | **Angle** |
| S7−Au1−S4 | 174.6(4) | S5−P1−S2 | 110.3(8) |
| S5−Au2−S4 | 174.1(5) | S5−P1−S4 | 105.8(7) |
| S3−Au3−S1 | 174.5(4) | S6−P2−S3 | 112.1(8) |
| S8−Au4−S2 | 172.3(5) | S7−P2−S3 | 113.4(7) |
| S7−Au5−S6 | 175.4(4) | S7−P2−S6 | 106.8(7) |
| P1−S1−Au3 | 101.3(6) | S8−P2−S3 | 115.6(8) |
| P1−S2−Au4 | 102.7(6) | S8−P2−S6 | 104.4(8) |
| P1−S4−Au1 | 96.1(6) | S8−P2−S7 | 103.6(8) |
| P1−S4−Au2 | 104.5(6) | P2−S3−Au3 | 102.3(7) |
| P1−S5−Au2 | 99.4(7) | P2−S6−Au5 | 94.5(7) |
| S2−P1−S1 | 120.5(8) | P2−S7−Au1 | 102.7(7) |
| S4−P1−S1 | 105.6(7) | P2−S7−Au5 | 58.3(6) |
| S4−P1−S2 | 108.8(7) | P2−S8−Au4 | 99.8(7) |
| S5−P1−S1 | 104.9(8) | | |

tronegativities: Au 2.2, Te 2.1) is the more electronegative partner compared to the chalcogen atom.

Metal−metal bonding is an additional point of interest in many coinage metal systems (M = Cu, Ag, Au)[6]. If the geometrical constraints of the ligand or the structure allow, many compounds show a tendency to cluster or polymerize. Such behaviour has been observed in many binary cluster compounds of the general types $[Au_m(PR)_{3m}]^{x+}$ and $[Au_{m+1}(PR_3)_m]^{y+}$[7], molecular alkylcopper compounds[8a], pentaazenidocopper complexes[8b], Hartl's iodocuprates[9], and in multinuclear copper chalcogenide clusters of the $Cu_{2n}Q_n(PR_3)_x$-type reported by Fenske and co-workers[10]. In many of these compounds, the metal−metal distances are comparable to, or are sometimes considerably shorter than, the M−M separations in the elemental metals. Thus, the obvious question arises[11] as to the nature of the interactions between metal centers at such short distances.

We have been intrigued by these questions and have studied the ternary and quaternary systems A/Au/Q (A = alkali metal; Q = S, Se, Te) and A/Au/B/Q (B = group 14 or 15 element). The use of electropositive cations such as alkali metal ions permits the stabilization of gold compounds with the relatively electronegative elements sulfur[12] and

Table 3. Crystal data, details of the data collection, and structure analysis of $K_2AuPS_4$ (**1**), $Tl_2AuPS_4$ (**2**), $K_2AuAsS_4$ (**3**), and $KAu_5P_2S_8$ (**4**)

| Empirical formula | $K_2AuPS_4$ | $Tl_2AuPS_4$ | $K_2AuAsS_4$ | $KAu_5P_2S_8$ |
|---|---|---|---|---|
| Formula weight | 434.4 | 764.9 | 478.3 | 1342.3 |
| Diffractometer | Siemens P4 | Siemens P4 | Siemens P4 | Nicolet P21 |
| Radiation | Mo-$K_\alpha$ | Mo-$K_\alpha$ | Mo-$K_\alpha$ | Mo-$K_\alpha$ |
| Monochromator | graphite | graphite | graphite | graphite |
| Data-collection mode | θ-2θ scan | θ-2θ scan | θ-2θ scan | ω scan |
| Crystal size [mm] | 0.2×0.12×0.06 | 0.3×0.1×0.06 | 0.15×0.08×0.04 | 0.3×0.04×0.04 |
| $T$ [K] | 203 | 198 | 198 | 293 |
| Wavelength | λ = 0.71073 | λ = 0.71073 | λ = 0.71073 | λ = 0.71073 |
| Crystal system | monoclinic | monoclinic | monoclinic | monoclinic |
| Space group | $P2_1/m$ | $P2_1/m$ | $P2_1/m$ | $P2_1/c$ |
| $a$ [Å] | 6.497(1) | 6.459(1) | 6.555(1) | 10.054(2) |
| $b$ [Å] | 6.727(1) | 6.669(1) | 6.859(1) | 13.464(3) |
| $c$ [Å] | 9.434(2) | 9.193(2) | 9.533(2) | 11.968(2) |
| β [°] | 92.69(3) | 93.84(3) | 92.64(3) | 106.16(3) |
| $V$ [Å$^3$] | 411.9(2) | 395.1(2) | 428.1(2) | 1556.2(5) |
| $Z$ | 2 | 2 | 2 | 4 |
| $D_{calcd.}$ [g/cm$^3$] | 3.502 | 6.43 | 3.711 | 5.729 |
| μ(Mo-$K_\alpha$)[mm$^{-1}$] | 19.975 | 60.358 | 22.868 | 48.485 |
| Absorption correction | semiempirical, Ψ scan, laminar (001) | semiempirical, Ψ scan, ellipsoid | semiempirical, Ψ scan, ellipsoid | semiempirical, Ψ scan, pseudoellipsoid |
| Min./max. transmission | 0.3752, 0.9311 | 0.290, 0.735 | 0.4841,0.5423 | 0.5546, 0.9825 |
| $F$(000) [e] | 392 | 640 | 428 | 2882 |
| θ range for data collection[°] | 4.0−54.0 | 4.0−54.0 | 4.0−54.0 | 4.0−54.0 |
| Index ranges | $-1 \le h \le 8$<br>$-8 \le k \le 8$<br>$-12 \le l \le 12$ | $-7 \le h \le 7$<br>$-8 \le k \le 8$<br>$-11 \le l \le 11$ | $-7 \le h \le 8$<br>$-1 \le k \le 8$<br>$-11 \le l \le 7$ | $0 \le h \le 12$<br>$-17 \le k \le 17$<br>$-15 \le l \le 14$ |
| Data collected | 2148 | 1969 | 1040 | 6147 |
| Unique data | 964 ($R_{int}$ = 0.046) | 924 ( $R_{int}$ = 0.042) | 767( $R_{int}$ = 0.054) | 3424 ($R_{int}$ = 0.126) |
| Observed data | 696 [$I > 2\sigma(I)$] | 784 [$I > 2\sigma(I)$] | 550 [$I > 2\sigma(I)$] | 1433 [$I > 3\sigma(I)$] |
| Refinement method | Full-matrix least squares on $F$ | Full-matrix least squares on $F$ | Full-matrix least squares on $F$ | Full-matrix least squares on $F$ |
| Parameters | 47 | 47 | 47 | 146 |
| Final $R$ indices [$I > 2\sigma(I)$] | $R$ = 0.0291 | $R$ = 0.0380 | $R$ = 0.0448 | $R$ = 0.0784 |
| | $Rw$ = 0.0627 | $Rw$ = 0.0959 | $Rw$ = 0.0923 | $Rw$ = 0.1028 |
| Goodness-of-Fit | 1.069 | 1.100 | 1.103 | 1.311 |
| Extinction coefficient | 0.0016(4) | 0.0124(8) | 0.0015(5) | 0.00038(4) |
| Largest diff. peak and hole [eÅ$^{-3}$] | 1.00; −1.40 | 2.66; −4.02 | 1.84; −1.61 | 3.25; −3.19 |

phosphorus. Thus, no ternary thiophosphates of Au exist. In contrast, for the lighter metals numerous compounds belonging to the ternary Ag−P−S[13] family have been reported in the literature, and some compounds of the type Cu−P−S[14] are known. Being itself rather electronegative, the usual, preferred chemistry for gold is through "soft" interactions with metalloids such as Te[15] and Bi[16].

In this paper, we report on two new thiophosphates of gold and an isostructural thioarsenate. A short account of this work has appeared elsewhere[17]. The compounds are $K_2AuPS_4$ (**1**), $Tl_2AuPS_4$ (**2**), $K_2AuAsS_4$ (**3**), and $KAu_5P_2S_8$ (**4**). During the preparation of this manuscript, one of the compounds presented here, $K_2AuPS_4$, was reported in the literature[18]. The compounds were prepared from Au, $A_2S$, S, and $P_2S_5$ or $As_2S_3$. The alkaline polythiophosphate or polythioarsenate forms a flux in situ. Kanatzidis and coworkers have used this feature to good advantage in the synthesis of metal thiophosphates such as $A_2AuP_2Se_6$ (A = K, Rb)[19], $A_2MP_2Se_6$ (A = K, Rb; M = Mn, Fe)[21], $A_2M_2P_2Se_6$ (A = K, Cs; M = Cu, Ag)[20], $A_3M(PS_4)_2$ (A = Rb, Cs; M = Sb, Bi)[20], as well as several main-group derivatives[21][22][23][24].

The structures of the title compounds have been determined by single-crystal X-ray diffraction techniques. Thermal and optical properties have also been investigated. One possible application of such compounds of the late transition metals stems from the fact that they have direct optical band gaps. Thus, they may be of interest in infra-red sensing. Also of interest is the observation of short Au−Au contacts in one of the compounds reported here.

## Results and Discussion

### Crystal Structures of $K_2AuPS_4$, $K_2AuAsS_4$, and $Tl_2AuPS_4$

Compounds **1**, **2**, and **3** are isostructural. Their structures consist of anionic columns separated by potassium cations, as shown in Figure 1. Selected distances and angles are compiled in Table 1. The $[AuPS_4]^{2-}$ columns run parallel to and are centered about the $b$ axis. In these chains, neighbouring $Au^I$ atoms are linked by $PS_4^{3-}$ tetrahedra in a *trans* orientation. The distances in **1** are as follows: The Au−S distance is 2.298(2) Å, comparable to that in KAuS [2.305(6) Å][12a], $Na_3AuS_2$ [2.301(7) Å][12b], and $K_4Au_6S_5$ [2.295(6) Å][12c]. The $PS_4$ tetrahedra are slightly distorted.

The average P−S distance is 2.047 Å, with the individual P−S distances ranging from 2.014 to 2.080 Å. The S−P−S angles fall in a narrow range between 103.7 and 115.7°. Two crystallographically distinct $K^+$ cations K(1) and K(2) are situated between the anionic fragments and are surrounded by 6 and 9 S atoms, respectively, with an average K−S distance of 3.347 Å.

In **2**, the mean As−S distance is 2.165 Å. The $AsS_4$ units are slightly distorted with S−As−S bond angles ranging from 103.3 to 115.7°. The Au−Au distance (3.43 Å) is slightly longer than that in the thiophosphate. All other distances and angles are in the same range as those in the thiophosphate.

#### $KAu_5P_2S_8$

Compound **4** crystallizes with a structure that is characterized by infinite anionic $[Au_5P_2S_8]^-$ chains and isolated $K^+$ cations. The angular chains extend along the [110] and [1$\bar{1}$0] direction, as shown in Figure 2. The anionic framework is built up from linear $AuS_2$ dumbbell units and $PS_4^{3-}$ tetrahedra, as shown in Figure 3. The edges of two $PS_4^{3-}$ tetrahedra are alternately connected by two and three $Au^+$ ions, to form eight-membered $P(SAuS)_2P$ rings. Each $PS_4^{3-}$ tetrahedron is linked to neighbouring tetrahedra by 5 Au atoms, so that S(4) and S(7) are coordinated by two Au atoms. These anionic chains interact with each other through close Au−Au $d^{10}$−$d^{10}$ contacts [Au(1)−Au(3) 2.961 Å, Au(2)−Au(3) 3.043 Å]. This is not the case in **1**, which has Au−Au contacts of 3.364 Å. The short Au−Au distances are remarkable, since no sulfide bridging ligands or other steric effects are present that might account for this behaviour. The Au−Au short contacts are classical $d^{10}$−$d^{10}$ interactions, which are also observed in KAuS[12d]. The intra-chain Au−Au distances are short, ranging from 3.035(2) [Au(1)−Au(3)] to 3.204(2) Å. A theoretical interpretation of the Au−Au bonding in terms of the electron localization function (ELF)[26] will be presented in a separate communication[27]. The Au atoms have a different number of homoatomic contacts. Au is almost linearly coordinated (∡ S−Au−S: 174.1−175.5°); the mean Au−S bond length is 2.31 Å, which is normal for linear $AuS_2$ fragments[12].

The structure contains two crystallographically distinct P sites. The $PS_4^{3-}$ tetrahedra have a slightly distorted geometry, with bond lengths varying from 2.0−2.15 Å [P(1)−S] and 2.0−2.12 Å [P(2)−S]; bond angles range from 104−116° for [∡ S−P(2)−S] and from 105−120° for [∡ S−P(1)−S]. The distortion arises because one edge of the $PS_4^{3-}$ tetrahedra has two Au neighbours, resulting in a longer P−S distance. The $K^+$ ions fill the voids in the structure. They are highly coordinated by seven K−S contacts in the range between 3.2 and 3.7 Å. Selected bond lengths and angles for **4** are given in Table 2.

#### Properties − Thermal Analysis

Differential thermal analysis (DTA) showed that **1**, **2**, and **4** melt congruently at 386, 412, and 394°C, respectively. Figure 4(a) shows the DSC trace obtained upon heating and cooling of the starting materials (polysulfide, $As_2S_3$, elements). The sharp exotherm near 100°C corresponds to the reaction leading to the clean product $K_2AuAsS_4$. The sharp exotherm at 386°C obtained upon cooling thus corresponds to the crystallization of molten $K_2AuAsS_4$. For comparison, Figure 4(b) shows the DSC trace (heating and cooling) of pure $K_2AuAsS_4$. Figure 4(c) shows the powder diffractogram of the products obtained from the in situ reaction in the DSC cell. The vertical lines mark expected peak positions of the $K_2AuAsS_4$ structure obtained from the single-crystal study.

Figure 4. a) DSC diagram of the starting compounds of $K_2AuAsS_4$ (**2**), b) DSC diagram of $K_2AuAsS_4$ (**2**), c) powder pattern after the DSC experiments

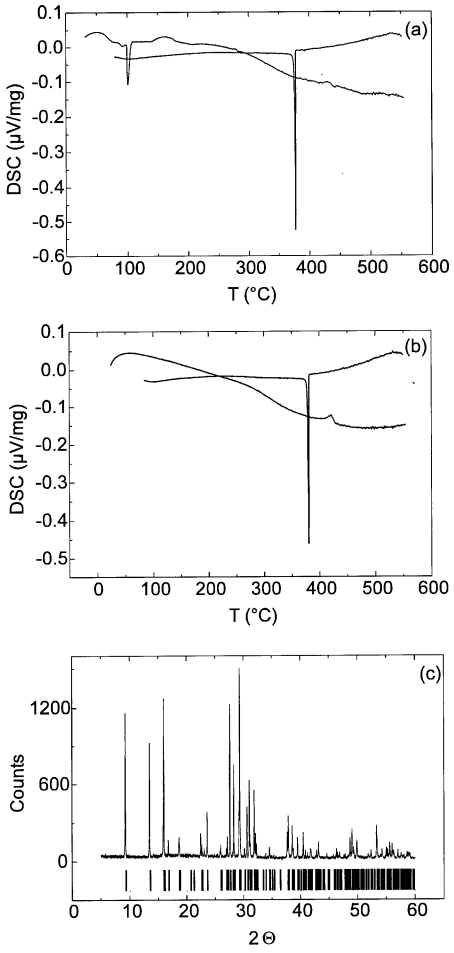


The optical absorption properties of the compounds **1**, **3**, and **4** were assessed by studying their UV/vis-near IR reflectance spectra. The spectra confirm the semiconducting nature of the materials by revealing the presence of abrupt optical gaps, as can be seen in Figure 5. The band gaps of **1** and **2** are 2.63 and 2.20 eV, respectively. Higher energy absorptions are readily resolved in these spectra and are assigned to electronic S→Au charge-transfer transitions. The band gap of **4** is found to be 2.14 eV.

The infrared spectra of the compounds are shown in Figure 6. The spectrum of **1** displays absorptions at ca. 613, ca. 557, ca. 521, ca. 471, ca. 397, ca. 370, ca. 272, ca. 245,

Figure 5. Plots of absorbance (arbitrary units) vs. energy (eV) for a) $K_2AuPS_4$ (**1**), b) $K_2AuAsS_4$ (**2**), and c) $KAu_5P_2S_8$ (**4**)

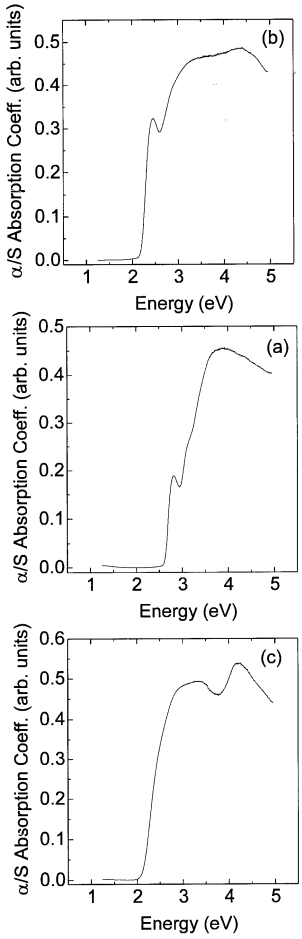


and ca. 228 $cm^{-1}$. The vibrations can mainly be assigned to $PS_4$ stretching modes by analogy with $Na_3PS_4 \cdot 8\ H_2O$[28]. The far-IR spectrum of **2** displays absorptions at ca. 459, ca. 430, ca. 401, ca. 392, ca. 353, ca. 314, ca. 293, and ca. 216 $cm^{-1}$. These values are shifted to lower energies in comparison with those of the thiophosphate because of the greater mass of As. Compound **4** exhibits absorptions at ca. 660, ca. 552, ca. 459, ca. 395, ca. 326, and ca. 236 $cm^{-1}$.

This research was supported by the *Fonds der Chemischen Industrie.* The donation of quartz tubes from *Heraeus Quarzschmelze* Hanau (Dr. *Höfer*) and of gold from *Degussa AG* is gratefully acknowledged. We are indebted to Dr. *Ram Seshadri* for fruitful discussions and a critical reading of the manuscript.

## Experimental Section

*Synthesis:* Starting materials were gold metal powder, $P_2S_5$ (Fluka, 99.99% purity, Alfa), $As_2S_3$ (Alfa, 99.998%), $K_2S$ and S powder (Riedel, 99.999%).

*Potassium Gold Thiophosphate, $K_2AuPS_4$* (**1**): A mixture of Au powder (0.164 g, 0.833 mmol), $K_2S$ (0.092 g, 0.833 mmol), $P_2S_5$ (0.093 g, 0.417 mmol), and S (0.013 g, 0.417 mmol) was loaded into a silica tube in a glovebox. The tube was evacuated and sealed in vacuo. The mixture was heated to 550°C over a period of 12 h and maintained at this temperature for 4 d. It was then allowed to cool slowly to room temperature at a rate of 4°C/h. The yellow, plate-like crystals thus obtained were found to be stable in air and insoluble both in water and in common organic solvents. The collected material was washed with water and then dried by rinsing with diethyl ether.

Figure 6. Far-IR spectra of a) $K_2AuPS_4$ (**1**), b) $K_2AuAsS_4$ (**2**), and c) $KAu_5P_2S_8$ (**4**)

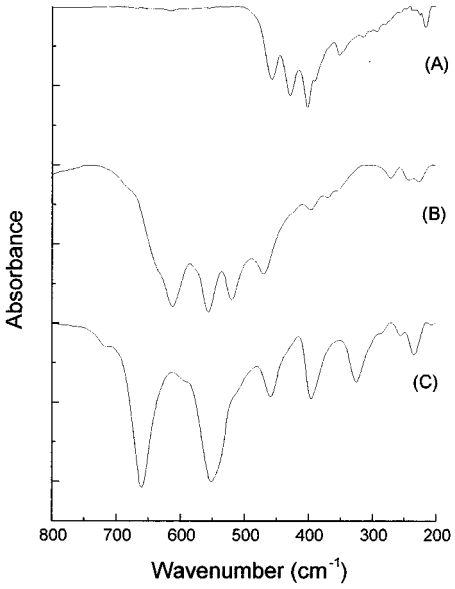


Table 4. Atomic coordinates and equivalent isotropic displacement parameters for $K_2AuPS_4$ (**1**) (with standard deviations in parentheses)

| Atom | *X* | *Y* | *Z* | *U*(eq)[a] |
|---|---|---|---|---|
| Au | 0 | 1/2 | 0 | 0.0197(1) |
| P | 0.2669(5) | 1/4 | 0.2804(4) | 0.0153(9) |
| K1 | 0.7959(5) | 1/4 | 0.4641(3) | 0.0221(8) |
| K2 | 0.4570(6) | 1/4 | 0.8346(4) | 0.032(1) |
| S1 | 0.9061(3) | 0.0054(6) | 0.7622(2) | 0.0223(5) |
| S2 | 0.5280(6) | 1/4 | 0.1738(4) | 0.023(1) |
| S3 | 0.3070(6) | 1/4 | 0.4939(3) | 0.0200(9) |

[a] The isotropic equivalent displacement parameter is defined as one-third of the trace of the orthogonalized $U_{ij}$ tensor.

Table 5. Atomic coordinates and equivalent isotropic displacement parameters for $Tl_2AuPS_4$ (**2**) (with standard deviations in parentheses)

| Atom | *X* | *Y* | *Z* | *U*(eq)[a] |
|---|---|---|---|---|
| Au | 0 | 1/2 | 0 | 0.0119(2) |
| P | 0.2843(8) | 1/4 | 0.7296(5) | 0.008(1) |
| Tl1 | 0.7896(1) | 1/4 | 0.54139(9) | 0.0162(3) |
| Tl2 | 0.4242(2) | 1/4 | 0.15382(9) | 0.0218(3) |
| S1 | 0.8824(6) | 0.4914(5) | 0.2306(4) | 0.0128(10) |
| S2 | 0.5623(9) | 1/4 | 0.8456(5) | 0.014(2) |
| S3 | 0.3020(8) | 1/4 | 0.5111(5) | 0.011(1) |

[a] The isotropic equivalent displacement parameter is defined as one-third of the trace of the orthogonalized $U_{ij}$ tensor.

Table 6. Atomic coordinates and equivalent isotropic displacement parameters for $K_2AuAsS_4$ (**3**) (with standard deviations in parentheses)

| Atom | *X* | *Y* | *Z* | *U*(eq)[a] |
|---|---|---|---|---|
| Au | 0 | 1/2 | 0 | 0.0190(3) |
| As | 0.2721(4) | 1/4 | 0.2802(3) | 0.0145(8) |
| K1 | 0.7977(8) | 1/4 | 0.4662(6) | 0.021(2) |
| K2 | 0.4537(10) | 1/4 | 0.8373(7) | 0.030(2) |
| S1 | 0.9079(6) | 0.0125(8) | 0.7653(5) | 0.025(1) |
| S2 | 0.550(1) | 1/4 | 0.1715(8) | 0.026(3) |
| S3 | 0.3071(10) | 1/4 | 0.5047(7) | 0.019(2) |

[a] The isotropic equivalent displacement parameter is defined as one-third of the trace of the orthogonalized $U_{ij}$ tensor.

Table 7. Atomic coordinates and equivalent isotropic displacement parameters for $KAu_5P_2S_8$ (**4**) (with standard deviations in parentheses)

| Atom | *X* | *Y* | *Z* | *U*(eq)[a] |
|---|---|---|---|---|
| Au1 | 0.2324(2) | 0.2618(1) | 0.0457(2) | 0.0226(7) |
| Au2 | 0.4382(2) | 0.4042(1) | −0.0710(2) | 0.0231(8) |
| Au3 | 0.2395(2) | 0.2447(2) | −0.1994(1) | 0.0194(7) |
| Au4 | 0.0586(2) | 0.0830(2) | −0.3585(2) | 0.0310(8) |
| Au5 | 0.1170(3) | 0.0473(2) | −0.0505(2) | 0.0360(9) |
| K1 | 0.309(1) | 0.7480(10) | 0.170(1) | 0.047(5) |
| S1 | 0.411(1) | 0.1233(9) | −0.1367(10) | 0.023(5) |
| S2 | 0.236(1) | −0.0171(9) | −0.378(1) | 0.027(5) |
| S3 | 0.079(2) | 0.3711(9) | −0.244(1) | 0.028(5) |
| S4 | 0.454(1) | 0.3266(9) | 0.105(1) | 0.025(5) |
| S5 | 0.423(2) | 0.465(1) | −0.254(1) | 0.041(6) |
| S6 | 0.236(1) | −0.095(1) | −0.069(1) | 0.041(5) |
| S7 | 0.013(2) | 0.197(1) | −0.032(1) | 0.037(5) |
| S8 | −0.136(1) | 0.177(1) | −0.364(1) | 0.038(6) |
| P1 | 0.408(2) | 0.0577(9) | −0.286(1) | 0.020(5) |
| P2 | 0.939(1) | 0.183(1) | 0.1170(9) | 0.027(5) |

[a] The isotropic equivalent displacement parameter is defined as one-third of the trace of the orthogonalized $U_{ij}$ tensor.

*Thallium Gold Thiophosphate, $Tl_2AuPS_4$* (**2**): Au powder (35 mg, 0.178 mmol), $Tl_2S$ (79 mg, 0.355 mmol), $P_2S_5$ (78 mg, 0.178 mmol), and S (57 mg, 1.778 mmol) were heated to 700°C over a period of 12 h and maintained at this temperature for 4 d. The mixture was then slowly cooled to room temperature at a rate of 4°C/h. The long, red plates thus obtained were found to be both air- and water-stable.

*Potassium Gold Thioarsenate, $K_2AuAsS_4$* (**3**): Pure material was obtained by heating a mixture of Au powder (0.123 g, 0.625 mmol), $K_2S$ (0.069 g, 0.625 mmol), $As_2S_3$ (0.077 g, 0.312 mmol), and S (0.03 g, 0.937 mmol) in analogy to the procedure described for **1**. Orange, plate-like crystals were formed, which were found to be slightly air-sensitive and which decomposed in water.

*Potassium Gold Thiophosphate, $KAu_5P_2S_8$* (**4**): 0.123 g (0.62 mmol) of Au, 0.034 g (0.31 mmol) of $K_2S$, 0.069 g (0.31 mmol) of $P_2S_5$, and 0.04 g (1.25 mmol) of S were heated as described above. Red, needle-shaped crystals were collected from the charge under inert atmosphere and were washed with anhydrous diethyl ether. The crystals were found to disintegrate in water or after exposure to air for 1 d.

*Structure Determination:* Crystal structures were determined from single-crystal X-ray diffraction data at 294 K for **4** and at 200 K for the other two compounds. A Siemens P4 diffractometer was used for the data collection. After Lorentz and polarization corrections, absorption corrections were made by acquiring Ψ scans and using the program XEMP in the SHELXTL package[29]. The structures were solved in the different space groups using direct methods with the package SHELXTL. Refinements were performed against $F_o^2$.using SHELXL-93[30]. Final refinement cycles included anisotropic thermal parameters on all atoms. Details of the data collection and refinement are given in Table 3. The final atomic and equivalent thermal parameters are listed in Tables 4−7. Further details of the crystal structure determinations may be obtained from the Fachinformatioszentrum Karlsruhe, D-76344 Eggenstein-Leopoldshafen (Germany), on quoting the depository numbers CSD-407912 ($K_2AuPS_4$), -407910 ($Tl_2AuPS_4$), -407913 ($K_2AuAsS_4$), and -407911 ($KAu_5P_2S_8$).

*Physical Measurements − Thermal Analysis:* Differential thermal analyses were performed with a Netzsch STA 429 thermal analyzer. Typically, samples of 30 mg of ground crystalline material were heated in quartz ampoules in vacuo. An empty quartz ampoule of equal mass was used as a reference. The samples were heated to the 600°C at a rate of 3°C/min and were then cooled to 50°C at the same rate. The DTA samples were examined by powder X-ray diffraction (D5000, Siemens) after the experiments.

*Optical Spectra:* UV/Vis/NIR spectra were acquired with a CARY 5 G (Varian) in the reflectance mode using a diffuse reflectance integrating sphere. The samples were diluted with $BaSO_4$.

*Infrared Spectra:* FT-IR spectra of samples pressed into KBr pellets were recorded with a Galaxy-2030 FT-IR spectrometer (Mattson Instruments).


[1] *Topics in Current Physics, Superconductivity in Ternary Compounds*, (Eds.: Ø. Fischer, M. B. Maple), Springer, Berlin, **1982**.
[2] J. A. Wilson, F. J. DiSalvo, S. Mahajan, *Adv. Phys.* **1975**, *24*, 117.
[3] [3a] M. S. Whittingham, A. J. Jacobson, *Intercalation Chemistry*, Academic Press, New York, **1982**. − [3b] R. H. Friend, A. D. Yoffe, *Adv. Phys.* **1987**, *36*, 1.
[4] [4a] J. Rouxel, *Chem. Eur. J.* **1996**, *2*, 1053. − [4b] M. Evain, *Eur. J. Solid State Inorg. Chem.* **1994**, *31*, 683. − [4c] S. Jobic, R. Brec, J. Rouxel, *J. Solid State Chem.* **1992**, *96*, 169. − [4d] S. Jobic, J. Rouxel, *J. Alloys Compd.* **1992**, *178*, 233. − [4e] S. Jobic, P. Deniard, R. Brec, J. Rouxel, A. Jouanneaux, A. Fitch, *Z. Anorg. Allg. Chem.* **1991**, *199*, 598.
[5] R. Hoffmann, C. Zheng, *J. Phys. Chem.* **1985**, *89*, 4175.
[6] *Unkonventionelle Wechselwirkungen in der Chemie metallischer Elemente* (Ed.: B. Krebs), VCH Publishers, Weinheim, **1992**.
[7] K. P. Hall, D. M. P. Mingos, *Prog. Inorg. Chem.* **1983**, *32*, 239.
[8] [8a] S. Gambarotta, C. Floriani, A. Chiesa-Villa, C. Guastini, *J. Chem. Soc., Chem. Commun.* **1983**, 1156. − [8b] J. Beck, J. Strähle, *Angew. Chem.* **1985**, *97*, 419; *Angew. Chem. Int. Ed. Engl.* **1985**, *24*, 409.
[9] H. Hartl, F. Mahdjour-Hassan-Abadi, *Angew. Chem.* **1984**, *96*, 359; *Angew. Chem. Int. Ed. Engl.* **1984**, *23*, 378; H. Hartl, F. Mahdjour-Hassan-Abadi, F. Fuchs, *Angew. Chem.* **1984**, *96*, 497; *Angew. Chem. Int. Ed. Engl.* **1984**, *23*, 514.
[10] D. Fenske in *Clusters and Colloids* (Ed.: G. Schmid), VCH Publishers, Weinheim, **1994**, pp. 212.
[11] [11a] P. K. Mehrotra, R. Hoffmann, *Inorg. Chem.* **1978**,*17*, 2187. − [11b] A. Dedieu, R. Hoffmann, *J. Am. Chem. Soc.* **1978**, *100*, 2074.
[12] See for example:
[12a] KAuS: K. O. Klepp, W. Bronger, *J. Less-Common Metals* **1987**, *127*, 65. − [12b] $Na_3AuS_2$: K. O. Klepp, W. Bronger, *J. Less-Common Metals* **1987**, *132*, 173. − [12c] $K_4Au_6S_5$: K. O. Klepp, W. Bronger, *J. Less-Common Metals* **1988**, *137*, 13. − [12d] $KAuS_5$: M. G. Kanatzidis, *Chem. Mater.* **1990**, *2*, 353. − [12e] AAuX (with A = Na, K, Rb, Cs; X = S, Se, Te): W. Bronger, H. U. Karthage, *J. Alloys Compd.* **1992**, *184*, 87.
[13] [13a] $AgPS_3$: P. Toffoli, P. Khodadad, N. Rodier, *Acta Crystallogr.* **1978**, *B34*, 3561. − [13b] $Ag_4P_2S_6$: P. Toffoli, P. Khodadad, N. Rodier, *Acta Crystallogr.* **1983**, *C39*, 1485; P. Toffoli, P.

Khodadad, N. Rodier, *Acta Crystallogr.* **1982**, *B38*, 2374. – [13c] $Ag_4P_2S_7$: P. Toffoli, P. Khodadad, N. Rodier, *Acta Crystallogr.* **1977**, *B33*, 1492. – [13d] $Ag_7PS_6$: R. Blachnik, U. Wickel, *Z. Naturforsch.* **1980**, *B35*, 1268. – [13e] $Ag_7P_3S_{11}$: P. Toffoli, P. Khodadad, N. Rodier, *Acta Crystallogr.* **1982**, *B38*, 2374.

[14] [14a] $CuPS_2$: J. K. Kom, J. Flahaut, L. Domange, *C. R. Seances Acad. Sci. Paris* **1963**, *257*, 3919. – [14b] $Cu_3PS_4$: R. Nitsche, P. Wild, *Mat. Res. Bull.* **1970**, *4*, 419; *J. Solid State Chem*. **1983**, *49*, 43.

[15] G. Tunell, L. Pauling, *Acta Crystallogr.* **1952**, *5*, 375.

[16] T. H. Geballe, V. B. Compton, *Rev. Mod. Phys.* **1963**, *35*, 1.

[17] S. Löken, W. Tremel, *12th International Conference on Solid Compounds of Transition Elements*, St. Malo, April 22−25, **1997**, Abstract P-D 49.

[18] K. Chondroudis, J. A. Hanko, M. G. Kanatzidis, *Inorg. Chem.* **1997**, *36*, 2623.

[19] K. Chondroudis, T. J. McCarthy, M. G. Kanatzidis, *Inorg. Chem.* **1996**, *35*, 3451.

[20] T. J. McCarthy, M. G. Kanatzidis, *J. Alloys Compd.* **1996**, *236*, 70.

[21] T. J. McCarthy, M. G. Kanatzidis, *Inorg. Chem.* **1995**, *34*, 1257; A. Sutorik, M. G. Kanatzidis, *Progr. Inorg. Chem.* **1995**, *43*, 151.

[22] T. J. McCarthy, M. G. Kanatzidis, *J. Chem. Soc., Chem. Commun.* **1994**, 1089.

[23] T. J. McCarthy, M. G. Kanatzidis, *Chem. Mater.* **1993**, *5*, 1061.

[24] K. Chondroudis, T. J. McCarthy, M. G. Kanatzidis, *Inorg. Chem.* **1996**, *35*, 840.

[25] K. Chondroudis, M. G. Kanatzidis, *Inorg. Chem.* **1995**, *34*, 5401.

[26] C. Felser, S. Löken, Y. Grin, W. Tremel, unpublished results.

[27] [27a] A. D. Becke, K. E. Edgecomb, *J. Chem. Phys.* **1990**, *92*, 5397. – [27b] B. Silvi, A. Savin. *Nature* **1994**, *371*, 683.

[28] A. Feltz, G. Pfaff, *Z. Anorg. Allg. Chem.* **1978**, *442*, 41.

[29] G. M. Sheldrick, Siemens Analytical X-ray Instruments Inc., Madison, WI, USA, **1991**.

[30] G. M. Sheldrick, *SHELXL 93, Program for the refinement of Crystal Structures*, Univerity of Göttingen, Germany, **1993**.

[97169]